$^{14}CO_2$ Processing and Measurement Activities at CU-INSTAAR and NOAA-ESRL

S.J. Lehman[1], P.P. Tans[2], J. B. Miller[2,3], S. A. Monzka[2], C. Sweeney[2,3], A. Andrews[2,3], J. C. Turnbull[4], J. Southon[5]

1. INSTAAR, University of Colorado, Boulder, CO USA 2. NOAA Earth System Research Laboratory, Boulder, CO USA 3. CIRES, U. Colorado, Boulder, CO USA 4. *now at:* Rafter Radiocarbon Laboratory, Lower Hutt NZ 5. Keck AMS Facility, University of California, Irvine CA USA

Contact: Scott.Lehman@Colorado.edu

An unbiased tracer of fossil fuel derived CO_2

Fossil fuel derived CO_2 (C_{ff}) is ^{14}C barren as a result of radioactive decay during storage of fossil carbon in the rock reservoir, while all other sources of CO_2 to the atmosphere are close in isotopic composition to the atmosphere itself. Simple mass balance considerations indicate a sensitivity of ambient $\Delta^{14}CO_2$ to addition of fossil fuel derived CO_2 of ~ -2.7 ‰/ppm. If other contributions to the tropospheric ^{14}C budget are either small or relatively uniform in space, then the mass balance sensitivity and the measurement precision will closely approximate the actual C_{ff} detection capability. As an indication of the strong relationship between ^{14}C and C_{ff} we compare in ***Figure 1*** maps of near-surface (~300 m) fossil fuel-derived CO_2 and total $\Delta^{14}CO_2$ over North America as represented by the TM5 transport model [*Krol et al.*, 2005]. The color scales depicting $\Delta^{14}CO_2$ and fossil fuel CO_2 distributions correspond to the expected mass balance sensitivity. Thus, the similar colors and patterns indicate that the ^{14}C gradients are controlled almost entirely by the presence of fossil fuel CO_2. The remaining small differences are due primarily to small atmospheric gradients imposed by the terrestrial disequilibrium flux, which is also quantified in the model. (This is the heterotrophic respiration of $^{14}CO_2$ photosynthetically assimilated a decade or two ago when the atmospheric $\Delta^{14}CO_2$ was much higher as a result of above-ground nuclear weapons testing.). Cosmogenic production and ocean disequilibrium isofluxes, which are important globally, do not result in significant spatial gradients of ^{14}C over the U.S., although they are also specified in the model.

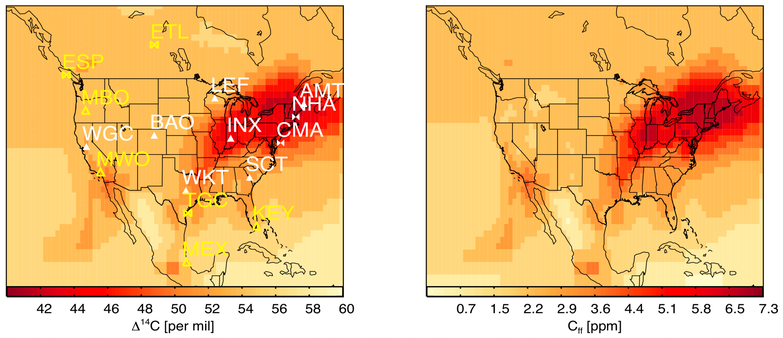

Figure 1. a) $\Delta^{14}CO_2$ (left panel) and b) the fossil fuel component of total CO_2 (C_{ff}; right panel) in the atmosphere near the surface over North America for a week in January of 2006 in the TM5 transport model. For comparison to simulated gradients, the long term $\Delta^{14}CO_2$ measurement error is 1.8‰ (1σ) (***Fig. 2***), equating to a C_{ff} detection of better than 1 ppm. The fossil fuel emissions used in the model are based on the CDIAC US and global totals and the spatial patterns from the EDGAR inventory (see carbontracker.noaa.gov). The sites labeled in white are existing ^{14}C sampling sites and those in yellow are planned sampling sites as needed to better characterize the "background" $\Delta^{14}CO_2$ (see ***eqs. 1b*** and ***c***) entering the coterminous U.S. Bowties are aircraft sites (three measurement altitudes each) and triangles are surface or tower sites. NWR (surface flask site) was excluded for clarity, but overlays with BAO.

$\Delta^{14}CO_2$ Measurement repeatability

Quantification of recently-added fossil fuel derived CO_2 (C_{ff}) requires measurements in both "background" and "observed" air for both the CO_2 mole fraction and its ^{14}C activity (i.e., ***eqs. 1a*** and ***b***), with the total uncertainty in C_{ff} dominated by the greater relative uncertainty of the $\Delta^{14}CO_2$ measurements. If the desired C_{ff} detection limit is 1 ppm (1σ), then the necessary $\Delta^{14}CO_2$ measurement precision will be ≤2 ‰ (1σ). At INSTAAR, the measurement repeatability is evaluated based on repeat extraction and measurement of whole air from control cylinders. Presently we measure 3 extraction aliquots from each of two cylinders, "NWT3" and "NWT4", in each AMS measurement wheel. Individual measurement wheels are comprised of 8 primary measurement standards, 2 secondary standards, 1 process blank (^{14}C-free air from cylinders), 6 controls, and 23 authentic samples. Extraction, graphitization, and measurement follow methods described in Turnbull *et al. [2007].* Extraction occurs on either a manual or an automated extraction line ("CRex", as described in Turnbull *et al., [2010]*) and samples from individual observing sites are always extracted on the same line. In ***Figure 2*** we show individual measurement values, means and un-normalized 1σ repeatabilities for both NWT3 and 4 by order of either measurement or extraction. There is no statistically significant difference between results for the two extraction lines. Temporal patterns of the measured value by measurement order suggest some systematic variances result from either graphitization or measurement conditions (graphitization and measurement occur nearly simultaneously). For authentic samples we report the un-normalized 1-sigma measurement repeatability of ±1.8 ‰ or the single sample measurement precision, whichever is greater. Long term repeatabilities for NWT3 and 4 are comparable to that for our previous control cylinder measured from 2003-2009, "NWTstd" [*Turnbull et al., 2007; Lehman et al., 2010*], which is near exhaustion. ***John Southon and colleagues at the UC-Irvine Keck AMS Facility are responsible for the high quality and stability of the measurements***.

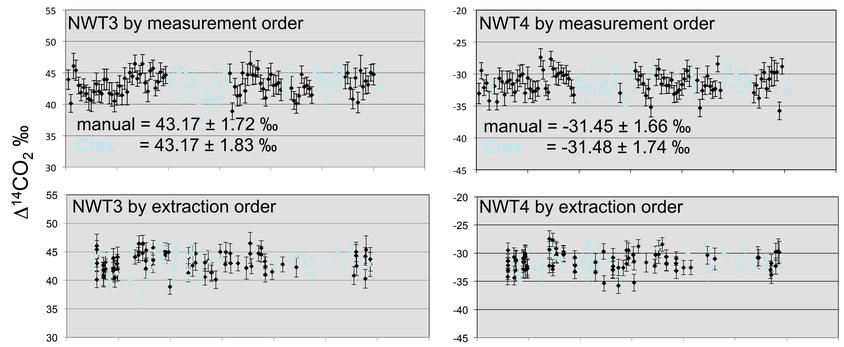

Figure 2. Measurement values for individual extraction aliquots of NWT3 (left panels) or NWT4 (right panels), by order of graphitization and measurement (top panels) or extraction (lower panels). High pressure control cylinders were prepared for INSTAAR from whole air collected at NOAA-ESRL's NWR site by Duane Kitzis. ^{14}C-free CO_2 was added to NWT4 to lower the activity.

For some of our observing sites (U.S. tall towers at BAO, LEF, and AMT in ***Figure 1a***) samples are extracted along with NWT3 and NWT4 at INSTAAR ("CRex" only) and graphitized and measured at LLNL-CAMS. INSTAAR-UCI and INSTAAR-CAMS measurement values agree within the standard error of the means (***Table 1***). Measurements were made over a period of ~2 years.

Table 1:	NWT3 (1s, n)	NWT4 (1s, n)
CRex-UCI	43.17‰ (1.83‰, 42)	-31.48‰ (1.74‰, 41)
CRex-CAMS	43.02‰ (2.34‰, 40)	-31.98‰ (2.08‰, 40)

Quantification of C_{ff}, NE U.S. example

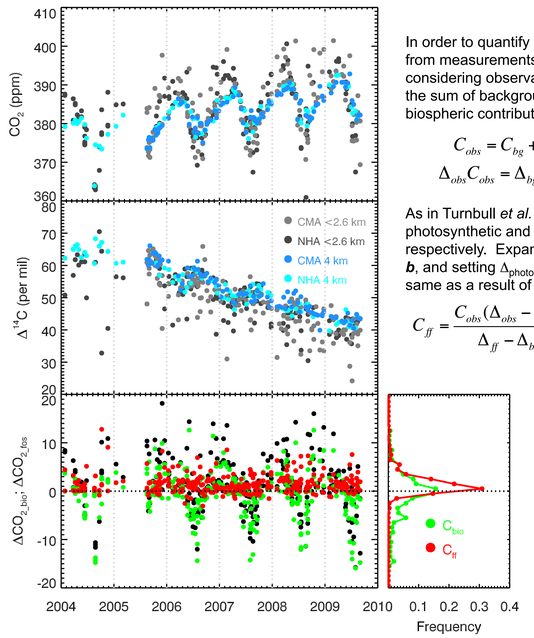

In order to quantify the fossil fuel CO_2 enhancement from measurements, we follow Levin *et al.* [2003] in considering observations of both CO_2 and $\Delta^{14}C$ to be the sum of background and any fossil fuel and biospheric contributions;

$$C_{obs} = C_{bg} + C_{ff} + C_{bio} \quad (1a)$$

$$\Delta_{obs}C_{obs} = \Delta_{bg}C_{bg} + \Delta_{ff}C_{ff} + \Delta_{bio}C_{bio} \quad (1b).$$

As in Turnbull *et al.* [2006], we divide C_{bio} into photosynthetic and respiratory terms, C_{photo} and C_{resp}, respectively. Expanding and combining ***eqs. 1a*** and ***b***, and setting Δ_{photo} equal to Δ_{bg} (which will be the same as a result of ^{13}C:^{12}C normalization), we obtain

$$C_{ff} = \frac{C_{obs}(\Delta_{obs} - \Delta_{bg})}{\Delta_{ff} - \Delta_{bg}} - \frac{C_{resp}(\Delta_{resp} - \Delta_{bg})}{\Delta_{ff} - \Delta_{bg}} \quad (1c).$$

In ***eq. 1c***, all of the quantities in the first term on the right-hand-side are either known *a priori* or can be measured, and the second term is a correction to C_{ff} that accounts for the disequilibrium contribution of ^{14}C from heterotrophic respiration which can be independently quantified.

Propagation of measurement uncertainties through ***eq. 1c*** indicates a C_{ff} detection limit of 1 ppm at 1σ.

Figure 3. CO_2 (top panel) and $\Delta^{14}C$ (middle panel) data from the aircraft sites CMA and NHA (***Fig. 1a***). 'Obs' (black and grey) are data from below 2600 m asl and 'bg' (blues) are data from above 2600 m. The lower panel shows the boundary layer enhancement or depletion of CO_2 (black) separated into the biogenic (green) and fossil (red) fractions, according to ***eqs. 1a*** and ***b***. The negative values of C_{ff} (histogram) arise from vertical $\Delta^{14}CO_2$ gradients that are within measurement uncertainties (***Fig. 2***) and from errors inherent in our one dimensional analytical model. **From** Miller *et al.*, [*submitted*].

Miller, J.B., **Lehman S.J.**, Montzka, S.A., Sweeney,C., Miller, B.R., Wolak, C., Miller, L., Dlugokencky, E.J., Southon, J., Turnbull, J.C. and P. P. Tans [submitted]. Linking emissions of fossil fuel CO_2 and other anthropogenic tracers using atmospheric $^{14}CO_2$. *Journal of Geophysical Research*.

Quantification of C_{ff}, E Asia example

China is now the world's largest emitter of fossil fuel derived CO_2, contributing more than 20% of global emissions. Emissions of other anthropogenic trace gases from E. Asia are also large and growing rapidly, and are often more poorly constrained than for CO_2. Carbon monoxide (CO) is of particular interest as it contributes to air pollution and is hazardous to human health. CO is produced as a by-product of combustion, and rapid economic development and increasing fossil fuel use in E. Asia, and particularly in China, would suggest an increase in CO emissions. However, concurrent improvements in combustion efficiency, replacement of older power plants, and a change from inefficient biomass combustion to fossil fuel use act to decrease CO emissions. The balance of these two competing effects is not yet clear.

We began observations in E. Asia in 2004. **Representative results presented here are all from Turnbull *et al.* [in press].**

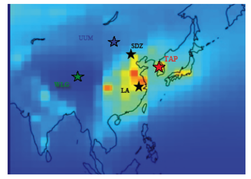

Figure 5. East Asia measurement sites (surface flask). Warm colors represent areas of regional $^{14}CO_2$ depletion and C_{ff} enhancement in the LMDZ transport model [from J. Turnbull].

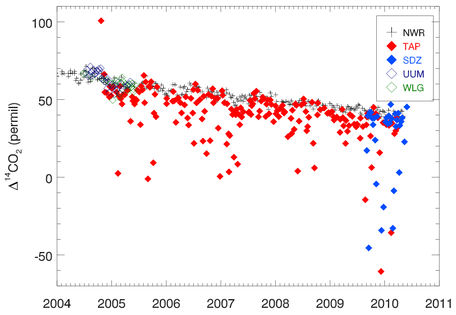

Figure 4. Time series of $\Delta^{14}CO_2$ from TAP (S. Korea), SDZ (NE PRC) along with observations from NWR, in the relatively clean well-mixed free troposphere in CO USA, and from two "remote" sites in Asia (WLG and UUM). Large depletions relative to NWR are evident for sites influenced by regional emissions of C_{ff} (***Fig. 5***).

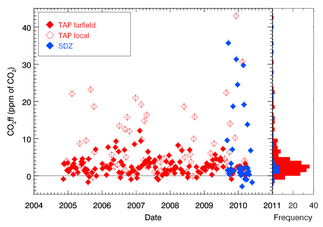

Figure 6. Estimates of C_{ff} for observations from TAP and SDZ. TAP results were divided into "far field" (PRC) and locally (S. Korea) influenced samples based on back trajectories and enhancements of SF_6. All from Turnbull *et al.*, [in press].

Turnbull, J.C., Tans, P.P, Lehman, S.J., Baker, D., Conway, T.J., Chung, Y.S., Gregg, J., Miller, J.B., Southon, J.R., and L-X. Zhou [in press]. Atmospheric observations of carbon monoxide and fossil fuel CO_2 emissions from East Asia. *Journal of Geophysical Research*.

$CO:C_{ff}$ emissions ratios, E Asia

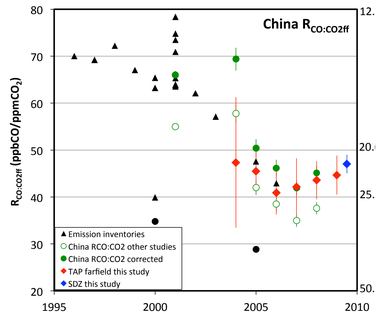

Figure 7. Comparison of CO:C_{ff} emissions ratios from our paired atmospheric observations of C_{ff} and CO (red), from prior atmospheric observations of CO and total CO_2 (green) and from emissions inventories (black). TAP C_{ff} is from annual averages of farfield observations in ***Fig. 6***. Correction of the previous observations was based on removal of the non-fossil CO_2 fraction based on our ^{14}C observations for the same year. From Turnbull *et al.*, [in press].

Additional references:

Lehman, S. J., J. B. Miller, J. C. Turnbull, J. R. Southon, P. P. Tans, and C. Sweeney (2011) $^{14}CO_2$ measurements in the NOAA/ESRL Global Co-operative Sampling Network: An update on measurements and data quality, in "*15th WMO/IAEA Meeting of Experts on Carbon Dioxide, Other Greenhouse Gases and Related Tracer Measurement Techniques (Jena, GDR 7-10 Sept. 2009)", World Meteorological Organization Global Atmosphere Watch Report No. 194*, W.A. Brand ed., pp. 315-318, Geneva CH.

Levin, I., B. Kromer, M. Schmidt, and H. Sartorius (2003), A novel approach for independent budgeting of fossil fuel CO2 over Europe by 14CO2 observations, *Geophys. Res. Lett.*, *30*(23), 2194.

Krol, M., S. Houweling, B. Bregman, M. van den Broek, A. Segers, P. van Velthoven, W. Peters, F. Dentener, and P. Bergamaschi (2005), The two-way nested global chemistry-transport zoom model TM5: algorithm and applications, *Atmospheric Chemistry and Physics*, *5*, 417-432.

Turnbull, J.C., Lehman, S.J., Morgan, S. and C. Wolak (2010) A new automated extraction system of 14C measurement in atmospheric CO_2. *Radiocarbon* 52_1261-9.

Turnbull, J.C., Lehman, S.J., Miller, J.B., Tans, P., Sparks, R.J., and J. Southon. (2007). A new high-precision $^{14}CO_2$ time series for North American continental air. *Journal of Geophysical Research* doi:10.1029/2006JD008184, 10 pp.

Turnbull, J.C., Miller, J.B., Lehman, S.J., Tans, P., Sparks, R.J., and J. Southon (2006). Comparison of $^{14}CO_2$, CO, and SF_6 as tracers for determination of recently added fossil fuel CO_2 in the atmosphere and implications for biological CO_2 exchange. *Geophysical Research Letters* 33, L01817, doi: 10.129/2005GL024213, 5 pp.

"*Ask and you shall receive*". UC-I's John Southon seeking guidance from above.